ELSEVIER

October 1995

Optical Materials 4 (1995) 791–795

OPTICAL Materials

Refractive indices of Zn-doped lithium niobate

U. Schlarb [a], M. Wöhlecke [a], B. Gather [b], A. Reichert [a], K. Betzler [a], T. Volk [c], N. Rubinina [d]

[a] *Fachbereich Physik, Universität Osnabrück, D 49069 Osnabrück, Germany*
[b] *Institut für Chemie, Universität Osnabrück, D 49069 Osnabrück, Germany*
[c] *Institute of Crystallography Russian Acad. Sci., Moscow 117333, Russia*
[d] *Moscow State University, 117234 Moscow, Russia*

Received 15 September 1994; accepted 15 November 1994

Abstract

We measured the index of refraction $n(\lambda)$ of Zn-doped $LiNbO_3$ grown from a congruent melt as a function of the Zn concentration in the crystal. The Zn concentration c_{Zn} in a sample was determined by electron microprobe technique. The refractive index $n(\lambda, c_{Zn})$ is described by a generalized Sellmeier equation for $400 < \lambda < 1200$ nm and c_{Zn} up to 8 mol% ZnO. Calculated phase-matching conditions of nonlinear effects like second-harmonic generation are in excellent agreement with experimental results obtained with the same set of crystals.

1. Introduction

Lithium niobate has a high potential for optical applications. Usually they require material with a distinct index of refraction and are often hampered by the photorefractive effect, also known as optical damage [1]. Both the refractive index and its sensitivity to light illumination are influenced by the crystal composition or – to be more specific – by the number of Nb antisites in the crystal [2]. Besides the techniques which improve the stoichiometry without any doping [3–5], several dopants like Mg [1], Zn [6], In [7] and Sc [8] are known to reduce the optical damage. While the growth of crystals with good optical homogeneity doped with one of the last two elements causes problems, samples of high optical quality are available up to approximately 9 mol% ZnO in the melt.

To explore and judge a large variety of possible applications we measured the refractive index over a wide wavelength and composition range and fitted the results to a generalized Sellmeier equation as described in detail recently for Mg doping [9]. The parameters for various second-harmonic generation (SHG) effects calculated with the aid of this equation are compared with experiments. The data are presented as a function of the Zn concentration c_{Zn} (mol% ZnO) in the crystals. Up to now only uncertain figures for the distribution coefficient of Zn in $LiNbO_3$ are published [10]. Therefore we determined more precise values using an electron microprobe.

2. Experimental details

The Zn-doped $LiNbO_3$ crystals were grown by the Czochralski technique from a congruent melt (48.5 mol% Li_2O and 51.5 mol% Nb_2O_5). Almost all specimens studied were cut from the boule center. The size of the samples was typically several mm in each dimension.

SSDI 0925-3467(95)00018-6

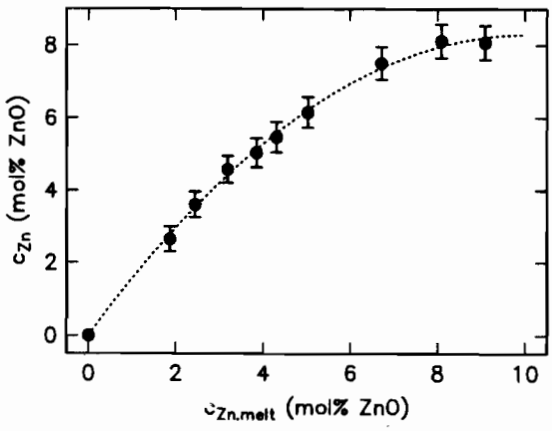

Fig. 1. Variation of the Zn concentration in the crystal c_{Zn} as a function of the mol% ZnO in the melt. The dotted curve represents a fit to these data with Eq. (1).

The compositions of the crystals were determined by electron microprobe analysis (Cameca SX 50 with wavelength dispersive spectrometers). For this purpose our set of optical measurement crystals was enlarged to improve the statistics. A Zn crystal and an undoped congruent $LiNbO_3$ sample served as standards for zinc, niobium and oxygen. The weight fractions have been transformed to mol fractions and were then normalized. This procedure avoids an increase of the scatter induced by lithium which is a very light element compared to niobium but contributes with a comparable mol fraction to $LiNbO_3$. For an easy comparison with properties only reported as a function of x mol% ZnO added to the melt we normalize the ZnO concentration according to x mol% ZnO/(48.5 mol% Li_2O + 51.5 mol% Nb_2O_5 + x mol% ZnO) and call it $C_{Zn,melt}$.

The correspondence between the Zn concentration c_{Zn} in the crystal and $c_{Zn,melt}$ is shown in Fig. 1. For more convenience we furnish the reader with the empirical equation

$$c_{Zn} = 1.649 c_{Zn,melt} - 0.082 c_{Zn,melt}^2 , \qquad (1)$$

valid for $c_{Zn,melt} \leq 9$ mol% ZnO. Each concentration is given in mol% ZnO. The errors in the determination of the Zn concentration are approximately $\pm 0.3...0.5$ mol% ZnO. Our results for Zn can be compared with Mg-doping, where a change of the distribution coefficient with the doping concentration was found also [11].

For the refractive index measurements we used an interferometric method, recently described in detail [12,13] which yields an accuracy of about $\Delta n = 5 \times 10^{-4}$, provided the optical homogeneity of the sample is sufficient. Homogeneity tests by means of spatially resolved SHG measurements show that the composition varies less than 0.05 mol% ZnO, a value well below the composition uncertainty. In addition the uniformity of the doping along the c-axis was established by a measured birefringence gradient of less than 3×10^{-6} per cm.

3. Results and discussion

Both the ordinary and the extraordinary index of refraction are shown in Fig. 2 for five selected wavelengths in the range 400–1200 nm as a function of the mol% ZnO in the crystal. The refractive index n_o varies monotonically while the graph for n_e exhibits a weak kink. The results can be well described by a generalized Sellmeier equation which takes into account the defect structure of Li-deficient $LiNbO_3$ with a divalent dopant (Mg or Zn). For details of the derivation the reader is referred to Schlarb and Betzler [9].

The generalized Sellmeier equation is defined as

$$n_i^2 = \frac{A_{0,i} + A_{Nb_{Li},i} c_{Nb_{Li}} + A_{Zn,i} c_{Zn}}{(\lambda_{0,i} + \mu_{0,i} F)^{-2} - \lambda^{-2}} - A_{IR,i} \lambda^2 + A_{UV}, \qquad (2)$$

with

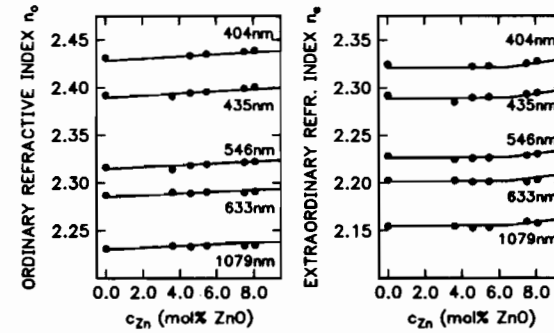

Fig. 2. Variation of the ordinary (n_o) and extraordinary (n_e) refractive index of congruently melting $LiNbO_3$ doped with Zn for selected wavelengths at room temperature. The lines are calculated with the generalized Sellmeier equation, experimental values are represented by dots.

Table 1
Parameters of the generalized Sellmeier equation. For the definition see Eq. (2) in the text

n_o	n_e
$\lambda_{0,o}=223.219$	$\lambda_{0,e}=218.203$
$\mu_{0,o}=1.1082\times10^{-6}$	$\mu_{0,e}=6.4047\times10^{-6}$
$A_{0,o}=4.5312\times10^{-5}$	$A_{0,e}=3.9466\times10^{-5}$
$A_{Nb_{Li},o}=-7.2320\times10^{-8}$	$A_{Nb_{Li},e}=11.8635\times10^{-7}$
$A_{Zn,o}=6.7963\times10^{-8}$	$A_{Zn,e}=1.9221\times10^{-7}$
$A_{IR,o}=3.6340\times10^{-8}$	$A_{IR,e}=3.0998\times10^{-8}$
$A_{UV}=2.6613$	$A_{UV}=2.6613$

$$c_{Nb_{Li}}=\begin{cases}\frac{2}{3}(50-c_{Li})-c_{Zn}/\alpha_{Zn} & \text{for } c_{Zn}<\alpha_{Zn}\frac{2}{3}(50-c_{Li})\\ 0 & \text{for } c_{Zn}\geq\alpha_{Zn}\frac{2}{3}(50-c_{Li})\end{cases}$$

$\alpha_{Zn}=6.5$;

$F=f(T)-f(T_0)$, $T_0=24.5°C$;

$$f(T)=(T+273)^2+4.0238\times10^5\left[\coth\left(\frac{261.6}{T+273}\right)-1\right].$$

c_{Li} denotes the initial Li content, i.e., the ratio $[Li_2O]/([Nb_2O_5]+[Li_2O])$ extrapolated to undoped material (measured in mol% Li_2O). The threshold concentration $c_{thr}=\alpha_{Zn}\frac{2}{3}(50-c_{Li})=6.5$ mol% ZnO for crystals grown from congruent melt was estimated from empirical results reported by Volk et al. [14] (The melt compositions given by the authors were normalized and converted to crystal compositions by Eq. (1)). The wavelength λ is given in nm, T in °C, and $i=e$ denotes the extraordinary, $i=o$ the ordinary light polarization.

Since all other parameters can be adopted from Ref. [9] it was only necessary to determine the parameters $A_{Zn,i}$ by a fit to our refractive index data as a function of wavelength and Zn concentration at room temperature. The standard deviation is about 1.8×10^{-3}. The numerical results for all parameters of the generalized Sellmeier equation are listed in Table 1.

Although the monotonic behavior of the ordinary refractive index and the weak kink of the extraordinary refractive index are shared with the corresponding properties of Mg-doped $LiNbO_3$, a remarkable difference is clearly observable for n_o. While n_o decreases with increasing Mg doping it increases in the case of Zn. Since Mg- and Zn-doped $LiNbO_3$ crystals have almost identical bandgaps this might be explained by the higher ionic radius of Zn^{2+} (83pm, Mg^{2+} 74pm) and its larger number of electrons: The transition matrix element for optical excitation is a measure of the overlap of the wave functions for the initial (p orbitals of oxygen) and final state (d-orbitals of Mg or Zn, respectively). A higher ionic radius causes a higher transition matrix element and therefore increases the refractive index.

We have put the Sellmeier equation to the proof by calculating the birefringence and comparing it with experimental data.The agreement demonstrated in Fig. 3 is convincing. The results exhibit a threshold in the Zn concentration, where the birefringence reaches a minimum. As mentioned above, the position of this threshold concentration at about 6.5 mol% ZnO is based upon empirical data and is not a result of the defect structure model used.

Nonlinear optical effects like noncolinear frequency doubling and phase matching due to a variation of the angle or temperature are governed by $n_o(\lambda)$ and $n_e(\lambda)$. This in turn allows us to calculate the corresponding data. As a test we measured the dependence of the type I phase matching angle on c_{Zn}. The results are shown in Fig. 4 for room temperature and a fundamental wavelength $\lambda_1=1064$ nm as open dots, the solid line is calculated from the equation

$$\frac{1}{n_o^2(\lambda_1)}=\frac{\cos^2\theta_{PM}}{n_o^2(\lambda_1/2)}+\frac{\sin^2\theta_{PM}}{n_e^2(\lambda_1/2)}, \quad (3)$$

where θ_{PM} denotes the direction of propagation in the crystal with respect to the optical axis. Since the [Li]/[Nb] ratio in the crystal may be influenced by the growth conditions and the Zn doping [15], we also

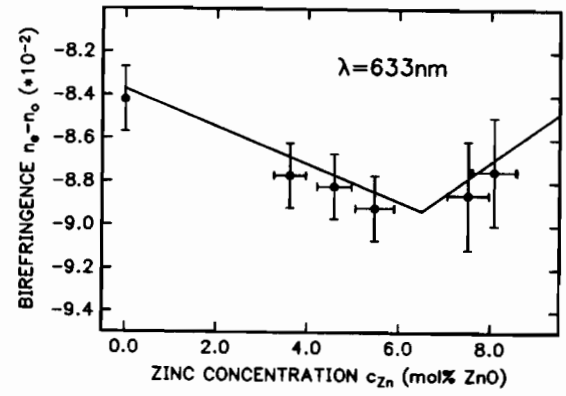

Fig. 3. Comparison of calculated (lines) and measured birefringence data of Zn-doped $LiNbO_3$ at room temperature for $\lambda=633$ nm.

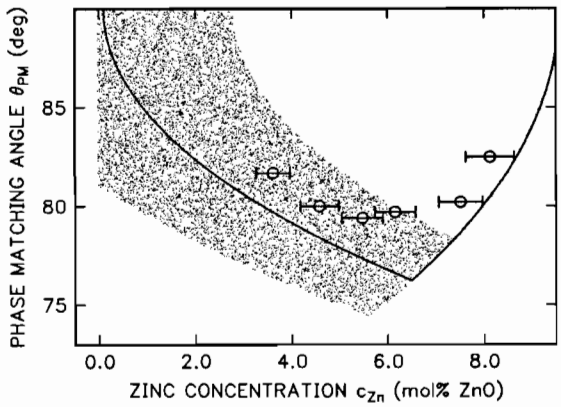

Fig. 4. Phase matching angle as a function of the crystal composition. The angles are measured inside the crystal with respect to the optical axis. The lines are calculated (see text). The grey shaded area corresponds to a variation in the initial Li-content in the crystal of $c_{Li} = 48.5 \pm 0.2$ mol% Li_2O.

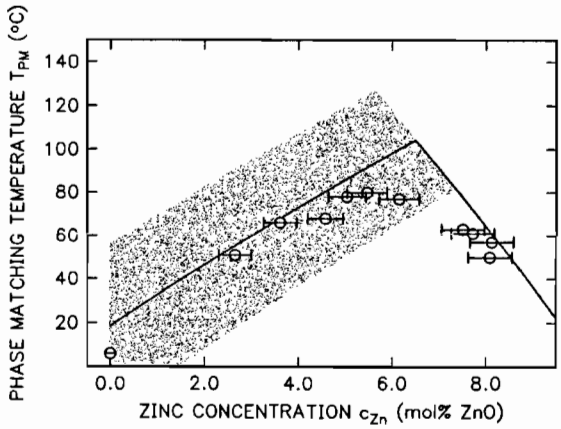

Fig. 5. Phase matching temperature of $LiNbO_3$:Zn as a function of the Zn concentration in the crystal for a fundamental wavelength of 1064nm. The curves are calculated from the generalized Sellmeier equation for an initial Li-content of $c_{Li} = 48.5 \pm 0.2$ mol% Li_2O (solid line and grey shaded area).

calculated the phase matching conditions for slightly different Li concentrations. Within a variation of ± 0.2 mol% Li_2O there is good correspondence with our measurements.In our simple model this variation has no effect at concentrations above the threshold value, because all Nb antisite defects are already replaced by Zn.

Although no temperature dependent refractive index data were used to determine the parameters $A_{Zn,i}$, the temperature variation of the refractive index of Zn-doped lithium niobate can be extrapolated from undoped material by the generalized Sellmeier equation with high accuracy. In the case of colinear noncritical type I second-harmonic generation (see Fig. 5), whose phase matching condition is given by

$$\Delta n_{SHG} = n_e(\lambda_1/2, T_{PM}) - n_o(\lambda_1, T_{PM}) = 0, \qquad (4)$$

the phase matching temperature T_{PM} can be computed for a given Li and Zn concentration. The calculations agree well with experimentals results, a maximum deviation of about 20°C is observed. This deviation allows us to estimate the error in the calculated refractive index. Neglecting the temperature variation of $n_o(1064\ \text{nm})$ and assuming $\partial n_e(532\ \text{nm})/\partial T \approx 1 \times 10^{-4}/°C$ yields $\Delta n = 0.002$ which is comparable to the standard deviation of the fit to room temperature refractive index data.

As a final example we present data on spontaneous noncolinear frequency doubling (SNCFD). In this technique the vectorial phase matching condition is obeyed by the fundamental beam and its Rayleigh scattered light, resulting in a cone of second harmonic radiation. Outside the crystal in a plane normal to the optic axis the cone angle $2\varphi_{SNCFD}$ is given by

$$\varphi_{SNCFD} = \arcsin\left(n_e(\lambda_1/2)\sqrt{1 - \frac{n_e^2(\lambda_1/2)}{n_o^2(\lambda_1)}}\right). \qquad (5)$$

Within a variation of ± 0.2 mol% Li_2O our calculations are in good agreement with experimental results (see Fig. 6).

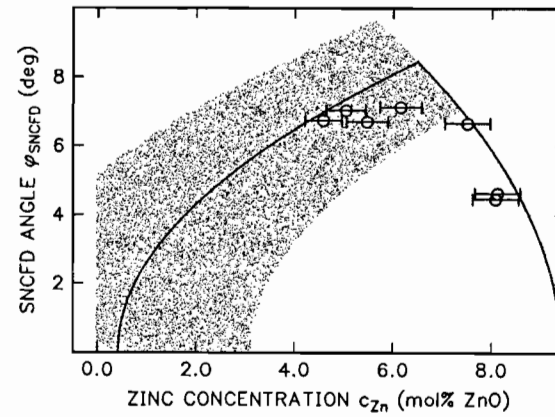

Fig. 6. Cone angle for spontaneous noncolinear frequency doubling as a function of the Zn concentration in the crystal. The curve is calculated using the generalized Sellmeier equation (see text) for a fundamental wavelength of 1064 nm, $T = 24.5$°C and an initial Li-content in the crystal $c_{Li} = 48.5 \pm 0.2$ mol% Li_2O (solid line and grey shaded area). Data points represent our measurements. The angles are measured outside the crystal in a plane normal to the optic axis.

The main differences of our results for Zn-doped material and Mg-doped lithium niobate (see Ref. [9]) are the higher threshold value (6.5 mol% ZnO versus 5 mol% MgO) and a slightly lower value for $|\Delta n_{SHG}|$ which leads, for example, to a slightly lower phase-matching temperature even at the threshold value.

4. Conclusion

We measured the refractive indices of $LiNbO_3$:Zn as a function of composition and wavelength. The results can be very well described by a previously proposed generalized Sellmeier equation, which takes into account the defect structure of Zn-doped $LiNbO_3$ in a simplified manner.

The generalized Sellmeier equation allows one to calculate the phase-matching conditions for all refractive-index-dependent effects in undoped and Zn-doped lithium niobate with excellent accuracy. Calculations of nonlinear effects like second-harmonic generation in $LiNbO_3$:Zn verify that the equation gives an accurate description of the refractive indices in the composition range from 0 to 8 mol% ZnO, in the wavelength range from 400 to 1200 nm and for temperatures between room temperature and at least 100°C. The maximum error in the calculated refractive indices is about 0.002.

Acknowledgements

Financial support from the Deutsche Forschungsgemeinschaft (SFB 225) is gratefully acknowledged.

References

[1] D.A. Bryan, R. Gerson and H.E. Tomaschke, Appl. Phys. Lett. 44 (1984) 847.
[2] O.F. Schirmer, O. Thiemann and M. Wöhlecke, J. Phys. Chem. Solids 52 (1991) 185.
[3] P.F. Bordui, R.G. Norwood, D.H. Jundt and M.M. Fejer, J. Appl. Phys. 71 (1992) 875.
[4] Y. Furukawa, M. Sato, K. Kitamura, Y. Yajima and M. Minakata, J. Appl. Phys. 72 (1992) 3250.
[5] G.I. Malovichko, V.G. Grachev, E.P. Kokanyan, O.F. Schirmer, K. Betzler, B. Gather, F. Jermann, S. Klauer, U. Schlarb and M. Wöhlecke, Appl. Phys. A 56 (1993) 103.
[6] T.R. Volk, V.I. Pryalkin and N.M. Rubinina, Optics Lett. 15 (1990) 996.
[7] T.R. Volk and N.M. Rubinina, Ferroel. Lett. 14 (1992) 37.
[8] J.K. Yamamoto, K. Kitamura, N. Iyi, S. Kimura, Y. Furukawa and M. Sato, Appl. Phys. Lett. 61 (1992) 2156.
[9] U. Schlarb and K. Betzler, Phys. Rev. B 50 (1994) 751.
[10] K. Nassau, in: Ferroelectricity, ed. E.F. Weller (Elsevier, Amsterdam, 1967) p. 259.
[11] L.J. Hu, Y.H. Chang, I.N. Lin and S.J. Yang, J. Cryst. Growth 114 (1991) 191.
[12] K. Betzler, A. Gröne, N. Schmidt and P. Voigt, Rev. Sci. Instrum. 59 (1988) 652.
[13] U. Schlarb and K. Betzler, Ferroelectrics 126 (1992) 39.
[14] T.R. Volk and N.M. Rubinina, Fiz. Tverd. Tela (Leningrad) 33 (1991) 1192, [Sov. Phys. Solid State 33 (1991) 674].
[15] Y.F. Zhou, J.C. Wang, W. Peiling, L.A. Tang, Q.B. Zhu, Y.A. Wu and H.R. Tan, J. Cryst. Growth 114 (1991) 87.